# The study about the transient characteristics of metallic fuel sodium cooled fast reactor in the unprotected loss of flow accident based on the SAS4A code

**Pengrui Qiao，Wenjun Hu**

China Institute of Atomic Energy, Beijing, China

*Presented by Error! Unknown document property name.*

**Abstract.** Unprotected loss of flow accident (ULOF) is the most typical severe accident in sodium cooled fast reactor, which is focused by scholars civil and abroad. Metallic fuel has different safety characteristics with the oxide fuel as the important development direction of future sodium fast reactor, accident analysis of which is also a research focus at home and abroad. This paper bases on one Cooperation Research Project proposed by ANL and organized by IAEA, analyses the Shut-down Removal Test-45R of the metallic fuel sodium cooled fast reactor EBR-II in the US with SAS4A code, to research the transient characteristics of it in ULOF accident. Studies have shown that, metallic fuel sodium cooled fast reactor has very good inherent safety performance, which can reduce the reactor power in ULOF accident through the negative feedback itself.

## 1. Introduction

With the rapid development of economy and society, people's demand for energy also continues to grow. As the largest developing country in the world, energy plays an important role in China's economic and social development. In the long term, nuclear energy as a safe, clean, economical energy, is an important direction to solve China's energy problems. As a preferred type of the fourth-generation nuclear energy system, the sodium-cooled fast reactor is an important part of the three-steps strategy of thermal reactor to fast reactor to fusion reactor[1], while the safety of sodium cooled fast reactor is being focused by researchers.

At present, MOX fuel and metallic fuel are both the fuel type choosed for sodium cooled fast reactor. The metallic fuel core and the oxide fuel core differ in the response state during the accident because of their different fuel property. For example, due to the good thermal conductivity of metallic fuel [2][3], the radial and axial distributions of the fuel rods are relatively flat, the center temperatures of the fuel rods are not very high, and the temperatures of the cladding and the coolant have no great difference with the fuel. In general, metallic fuels will be an important future direction for future sodium cooled fast reactors due to their high multiplicity, good heat transfer, good compatibility with sodium, and the ability to form closed fuel cycles. Therefore, we need to study the safety characteristics of metallic-fueled sodium cooled fast reactors.

The safety analysis of sodium cooled fast reactors is mainly focused on serious accidents of unprotected overpower, unprotected loss of flow and unprotected loss of heat sink which could lead to destructive disintegration of the core[4]. Wherein, the accident protection shutdown system fails to act properly due to mechanical failures or mishandling after loss of flow accident occurs, the reactor can only react passively on its own inherent safety mechanisms. As the volumetric power density of the sodium cooled fast reactor is large, the unprotected loss of flow accident is more serious than the transient overpower and the loss of heat sink accident in the fast reactor. Therefore, it is necessary to study the transient characteristics of the unprotected loss of flow accident of the sodium cooled fast reactor, so as to provide suggestions and reference for the safety function design and inherent safety improvement of the fast reactor.

ANL (Argonne National Laboratory) presented a benchmark based on the EBR-II reactor, coordinated by IAEA as an international coordination research project. China Institute of Atomic Energy is one of the participating members. The benchmark are about the problems of the SHRT-17 and SHRT-45R conducted at the experimental fast breeder reactor EBR-II[5]. The Shut-down Removal Test-45R of EBR-II is analyzed with SAS4A code, to research the transient characteristics of it in ULOF accident.

## 2. Brief introduction of EBR-II reactor

The EBR-II reactor is part of the Integrated Reactor Development and Verification Program for United States,it is a liquid metallic cooled fast reactor that the US Department of Energy authorized the Argonne National Laboratory for the construction and operation[6]. The heat power of EBR-II is 62.5MW with an electric power of 20MW, using sodium as a coolant, utilizing U-5Fs metallic fuel. Fig.1 shows a simplified diagram of the EBR-II reactor. EBR-II reactor has a characteristic of mixed-type reactor because of its heat transfer system. The flow path from the main pump to the IHX through the reactor is connected by piping, which is a similar configuration to a loop-type fast reactor. The outlet of the intermediate heat

exchanger, however, is not directly connected to the main pump but instead dicharges into a large cold pool. All of components, pumps, pipes, and the reactor core are in the sodium pool.

## 3. Procedure and model

### *3.1. Procedure Introduction*

In this paper, the SAS4A code is used as a tool for simulation analysis. The SAS4A code was developed at Argonne National Laboratory for the analysis of severe accidents in liquid metallic cooled reactors [7][8]. SAS4A has extensive capabilities for the analysis of severe accidents, including both theoretical models describing the fuel, cladding and coolant performance and experimental knowledge obtained from experiments. The code was designed to analyze the initiating phase of core disruptive accidents resulting from under-cooling or overpower conditions. SAS4A contains detailed, mechanistic models of transient thermal, hydraulic, neurotics, and fuel-pin mechanical effects. It computes fuel/cladding/coolant heating, coolant boiling, cladding failure as well as fuel/cladding melting and relocation.

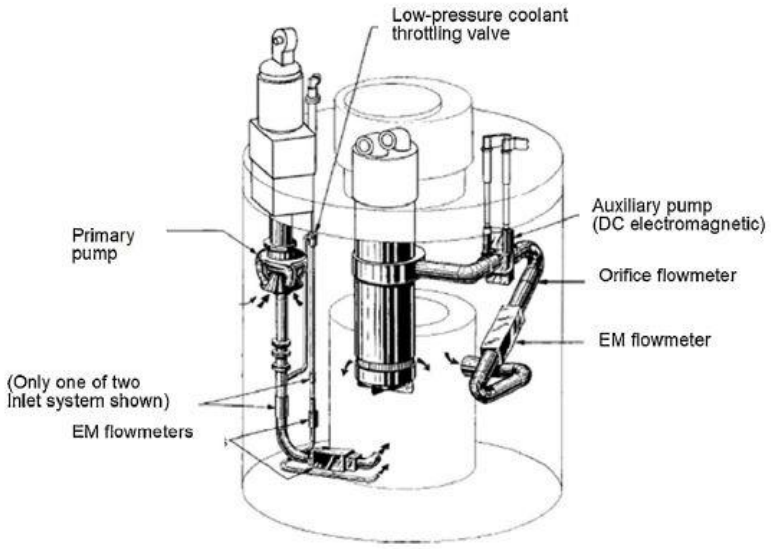


*Fig.1 Schematic of EBR-II reactor[5]*

### *3.2. Core modeling*

Fig.2 shows the core configuration of EBR-II for SHRT-45R test(drawn refer to the core model figure from [5]). As can be seen from the figure, the EBR-II core configuration is very complex, with many types of assemblies such as fuel assemblies, control rod assemblies, blanket assemblies, different test assemblies, measurement assemblies, and so on.

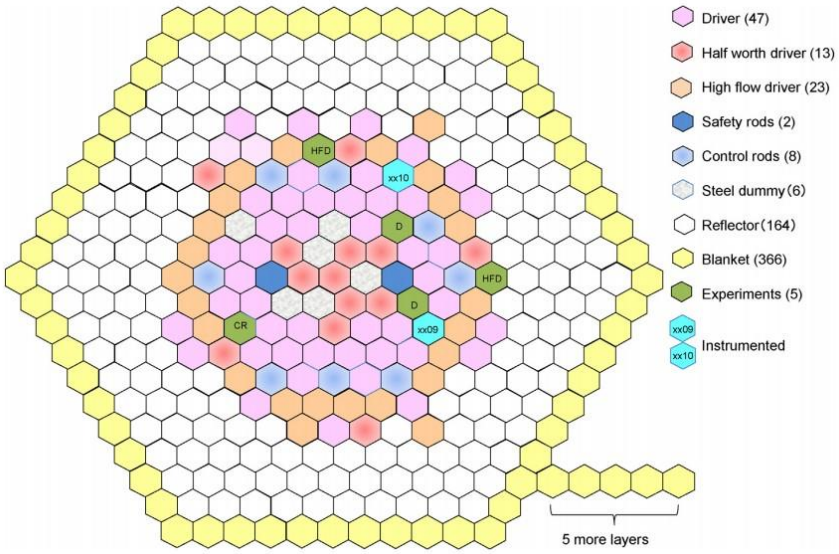


*Fig.2 Core configuration of EBR-II for SHRT-45R test*

In the ULOF accident, the response state of the core is extremely important, therefore, the core of EBR-II is simulated in detail, which is divided into 13 channels. Table.1 shows the core model patameters.

Table.1 Core model parameters

| **Channel number** | **Assembly type** | **Amount** | **Average Power（kW）** | **Average Flow（kg/s）** | **Power-to-flow ratio（kW・s/kg）** |
|---|---|---|---|---|---|
| 1 | hot driver | 1 | 715.7 | 63.55 | 9.16 |
| 2 | inner core driver(MARK-II A row3-5) | 17 | 652.9 | 89.57 | 7.33 |
| 3 | inner core driver(MARK-II AI row3-5) | 16 | 641.7 | 89.5 | 7.17 |
| 4 | external core driver(MARK-II A row6-7) | 15 | 590.2 | 68.94 | 8.57 |
| 5 | external core driver(MARK-II AI row6-7) | 25 | 542.6 | 66.64 | 8.14 |
| 6 | partial driver(MARK-II A row1-7) | 12 | 314.9 | 60.71 | 5.19 |
| 7 | control rod and safety rod | 10 | 430.6 | 65.09 | 6.62 |
| 8 | steel | 8 | 18.65 | 12.56 | 1.48 |

| | | | | | |
|---|---|---|---|---|---|
| 9 | reflector(row13-16) | 36 | 0.5858 | 1.006 | 0.58 |
| 10 | reflector(row7-10) | 165 | 8.225 | 1.429 | 5.76 |
| 11 | blanket | 330 | 16.24 | 3.632 | 4.47 |
| 12 | instrument(xx09) | 1 | 379.8 | 48.13 | 7.89 |
| 13 | instrument(xx10) | 1 | 18.31 | 6.768 | 2.71 |

### *3.3. Physical calculation*

Fast neutron reactors usually has compact structure, the time-space distribution of neutron flux density is more easily separated. Therefore, the point dynamic model is adopted:

$$\varphi(\mathrm{t}) = \varphi(\mathrm{t})\frac{\delta k(t)-\beta}{\Lambda} + \sum_i \lambda_i C_i(\mathrm{t}) \tag{1}$$

Where $\varphi(t)$ is the nominalized power

The net change rate of the delayed-onset neutron precursor is given by the following equation:

$$\dot{C}_i(\mathrm{t}) = \beta_i \varphi(\mathrm{t}) / \Lambda - \lambda_i C_i(\mathrm{t}) \tag{2}$$

where

$C_i(0) = \beta_i / \lambda_i \Lambda$

$\beta = \sum_i \beta_i$

$\delta k(t)$ total reactivity

$\beta$ total effective delayed neutron fraction

$\Lambda$ Neutron generation time

$\lambda_i$ decay constant of the delayed precursor neutron

In this work, six groups of delayed neutrons are used, and the feedback of fuel doppler effect, coolant density change, axial expansion and radial expansion are considered.

In SAS4A code, different channels have different decay thermal characteristics, and different decay heat curve is used in the different channels. Each decay thermal characteristic is given by the following equation:

$$\frac{dh_{nk}}{dt} = \beta_{hnk}\varphi(\mathrm{t}) - \lambda_{hnk}h_{nk} \tag{3}$$

Where

$h_{nk}$ nominalized decay heat energy fraction for group n of curve k

$\beta_{hnk}$ effective decay-heat group n power fraction for curve k

$\lambda_{hnk}$ decay-heat group effective decay constant for group n for curve k

$\varphi$ nominalized power level

In this work, Six typical decay heat models were selected. Specific physical calculation parameters are in Table.2.

Table.2 Physical parameters

| $\beta_i$ | $\lambda_i$ | $\beta_{hnk}$ | $\lambda_{hnk}$ |
|---|---|---|---|
| 2.19E-04 | 1.27E-02 | 2.50E-02 | 9.18E-02 |
| 1.33E-03 | 3.17E-02 | 1.76E-02 | 6.83E-03 |
| 1.23E-03 | 1.15E-01 | 1.34E-02 | 4.81E-04 |
| 2.69E-03 | 3.11E-01 | 6.70E-03 | 4.58E-05 |
| 9.90E-04 | 1.40E+00 | 3.56E-03 | 3.34E-06 |
| 2.43E-04 | 3.87E+00 | 3.33E-03 | 1.07E-11 |

### *3.4. Thermal-hydraulics calculation*

In SAS4A code, the basic transient heat transfer equations for fuel and cladding are given below:

$$r c \frac{\P T}{\P t} = \frac{1}{r}\frac{\P}{\P r}(\mathrm{k}\, r \frac{\P T}{\P t}) + Q \tag{4}$$

Where

$\rho$ density

k thermal conductivity

c Specific heat

The basic heat transfer equation for the coolant is as follows:

$$r cA_c \frac{\P T}{\P t} + \frac{\P}{\P r}(wcT) = (Q_c + Q_{ec} + Q_{sc})A_c \quad (5)$$

where

$A_c$ coolant flow area, is given in geometric modeling

$w$ coolant mass flow rate

$Q_c$ heat generated by coolant

$Q_{ec}$ heat flow from clad to coolant

$Q_{sc}$ heat flow from structure to coolant

$$Q_c = \frac{g_c \bar{P}(\mathrm{j})}{A_c \mathrm{D}z(\mathrm{j})}$$

where

$P(\mathrm{j})$ total heat generated at the axial node j

$\mathrm{D}z(\mathrm{j})$ height of the axial node j

## 4. Simulation Calculation and Analysis

### *4.1. Steady - state calculation*

The steady-state calculation is carried out for the core model established in chapter 3.2. The input data for steady state calculation is shown in Table.3.

Table.3 Input parameters for steady state calculation

| **Parameters** | **unit** | **value** |
|---|---|---|
| Core thermal power | MW | 62.5 |
| Core inlet coolant average temperature | K | 624 |
| Core outlet coolant average temperature | K | 746 |

The steady-state calculation results are shown in Table.4.

Table.4 Steady-state calculation results

| **Channel Number** | **peak fuel temperature（K）** | **Peak cladding temperature（K）** | **Outlet Coolant temperature（K）** |
|---|---|---|---|
| 1 | 840.11 | 777.19 | 758.26 |
| 2 | 823.85 | 750.66 | 727.89 |
| 3 | 821.38 | 749.72 | 727.53 |
| 4 | 835.40 | 769.28 | 749.14 |
| 5 | 824.39 | 761.48 | 742.50 |
| 6 | 796.01 | 721.33 | 696.76 |
| 7 | 698.04 | 662.81 | 651.87 |
| 8 | 690.43 | 667.11 | 639.48 |
| 9 | 633.42 | 630.14 | 625.64 |
| 10 | 818.87 | 777.63 | 705.24 |
| 11 | 685.83 | 685.16 | 685.40 |
| 12 | 827.00 | 759.56 | 738.63 |
| 13 | 677.62 | 667.40 | 658.21 |

As we can see in Table.4, Channel 1 (hottest component) has the highest fuel temperature of 840.11K, the highest cladding temperature of 777.19k, the highest coolant temperature of 758.26K. The coolant outlet temperature of each channel of steady state calculation are in line with the core design parameters, the temperature profile of channels also matches the power and flow distribution of the reactor core. The correctness of core model is preliminarily verified.

### *4.2. Transient calculation*

In ULOF accident simulation, we consider the accident trigger is the failure of primary loop pump, where the pump power P(t) coasts down by the following relation:

$$Q = \frac{Q_0}{1 + t / t_h} \tag{6}$$

where

$Q_0$ initial flowrate (flowrate of steady state)

$t$ time after accident started

$t_h$ pump coast down half time

The main assumptions used in the accident are as followed:

1) Accident starts at 0s

2) Before the accident, the reactor was in a state of 100% rated power, and the flow rate of the reactor was 100%

3) During the accident, the emergency shutdown system does not act

4) The calculation boundary condition of the accident is the change of the pressure head (nominalized value) for the core coolant inlet with time, as shown in Fig.3.

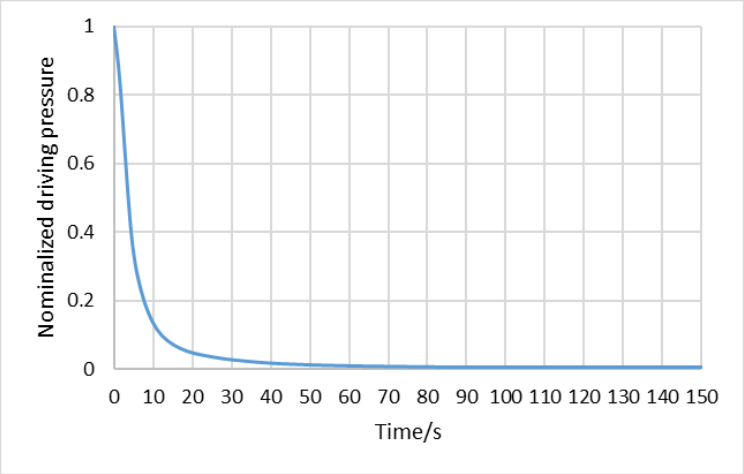


*Fig.3 Curve of the nominalized pressure head in the core coolant inlet varied with time*

The relative power, relative flow rate and relative power-to-flow ratio of EBR-II under the condition of unprotected loss of flow are obtained, as shown in Fig.4. Reactivity verification are shown in Fig.5. The peak temperature of the fuel, cladding and coolant in the hottest channel is shown in Fig.6.

At the beginning of the accident, because the pump stops running, core flow decreased rapidly, which lead to a rise in power-to-flow ratio. Due to the good thermal conductivity of metallic fuel, the core coolant temperature of the reactor is increased rapidly, and the negative reactivity is introduced into the reactor, which leads to the decrease of the core power.The power-flow ratio reaches maximum value 2.5 times the rated power-flow ratio at 55s, after that the reactor core power declines more rapidly than the core flow, power-to-flow ratio is reduced, and eventually tends to be stable, at about 1.0 times rated power-to-flow ratio.

Net reactivity feedback reached the maximum value (-0.334$) at 53s, and then the net reactivity feedback gradually decreases and eventually tends to zero.

As can be seen from Fig.5, in the whole transient process, all of the reactivity caused by coolant density change, axial expansion, radial expansion and the doppler effect are negative, wherein, the sodium density change has brought the largest negative feedback, the maximum value of which is -0.18$. The smallest feedback contribution is brought by the doppler effect of the reactivity, which is in the $10^{-3}$ level, and has little effect on the accident process. Because the size of EBR-II reactor is small, when the temperature of the coolant increases, the sodium density decreases, bringing the neutron leakage rate increases, which introduces a large negative feedback. In the large-scale fast reactor, the sodium voiding effect of th are generally positive feedback, when designing a reactor, the positive sodium voiding reactivity feedback should be minimized.

As can be seen from Fig.6, the peak temperature of the fuel, cladding and coolant temperature increase with the change of the power-to-flow ratio, and then decreases, finally tends to be stable. The peak temperature of the fuel, the cladding and the coolant reaches the maximum value of 922K, 914K, 912K respectively at 55s. The fuel and cladding does not melt and the coolant does not boil. The coolant temperature is higher than that of fuel after 55s, which seems not in logic, the reason may be that the circuit is not model, and the temperature of fuel decreased faster than the coolant.

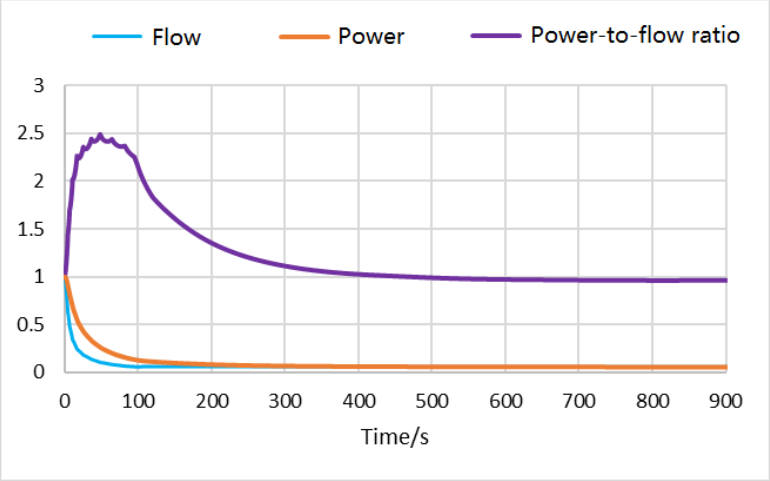


*Fig.4 Nominalized power, flow, power flow ratio changes with time*

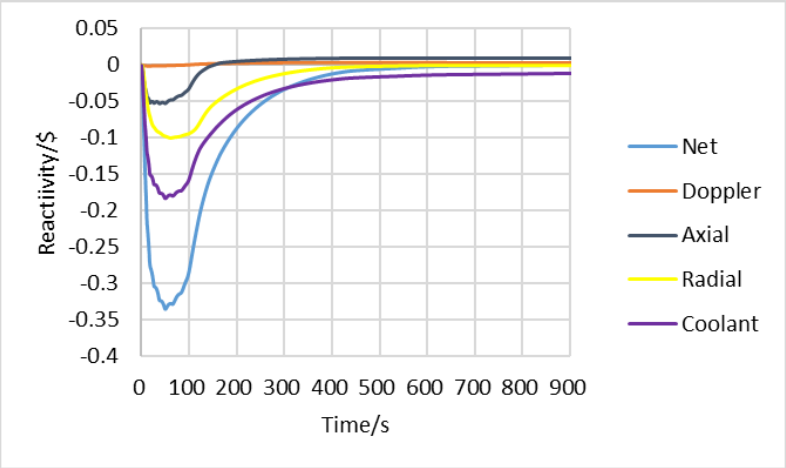


*Fig.5 Reactive feedback change with time*

In order to illustrate the correctness of the results, the results of this paper are compared with the results of ANL and the measured values, as shown in Fig. 7 ~ Fig.9. ANL also used SAS4A procedures for calculation. However, ANL established a complete second and third circuit model, this paper only build a simple core primary loop model. The SHRT-45R test

gives the measured values of the main pump flow, fission power, and the temperature and flow of the instrument subassembly XX09.

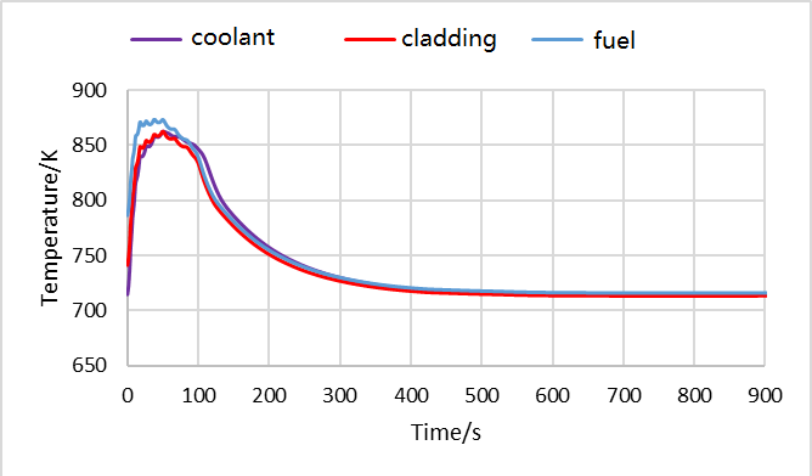


*Fig.6 Peak temperature of fuel, cladding and coolant in hottest channel change with time*

Fig.7 shows the fission power change with time. Before 200s, the results of the three agree very well. After 200s, the calculated results are slightly higher than the experimental results, result of ANL shows the same trend, but in general the difference is not great, within a reasonable range. Fig.8 shows the relative flow rate with time, it can be seen from the figure that the calculated results in this paper and the results of ANL calculations are both in good agreement with experimental measurements.

Fig.9 shows the temperature change over time at the outlet of the XX09 channel. It can be seen in the figure that the calculated results are in good agreement with the experimental results in the first 400 s. After 400 s, the calculated results are gradually higher than the experimental results. The final stable temperature has a difference of about 30 K. By comparing the results of this paper with the results of ANL, it is found that the calculated results are consistent with that of ANL (data is from the result submitted by ANL to the CRP work group), and the final stable temperature is almost the same, but the result of ANL at the peak is obviously lower than that calculated in this paper about 50K. In order to compare the results of the calculation more clearly, the result of Terra Power (TP) (data is from the result submitted by TP to the CRP work group) is introduced, which also calculated with SAS4A code. It can be seen from the figure that the calculated results of Terra Power are in good agreement with the calculated results in this paper, and the results are in good agreement with the experimental results. It can be seen from the figure that the core outlet temperature eventually tends to the initial value, proving that the reactor core power and the natural circulation flow match each other under the effect of reactive feedback, leading the temperature difference between the inlet and outlet to return to the initial value.

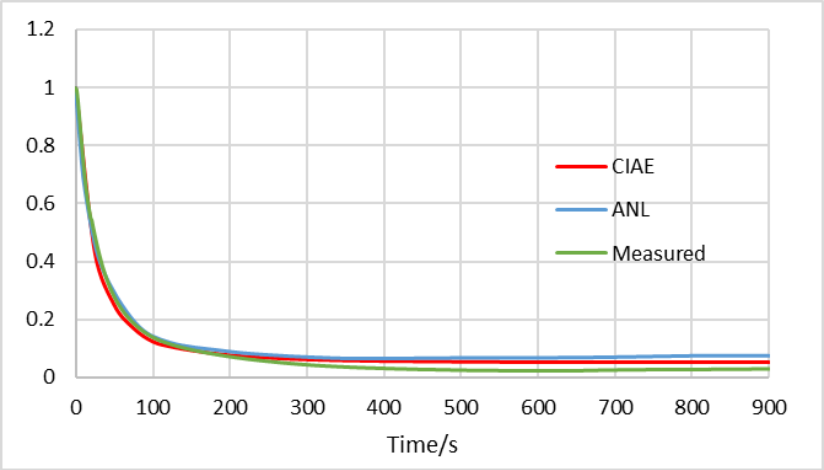


*Fig.7 Fission power of results for CIAE，ANL and experiment measured*

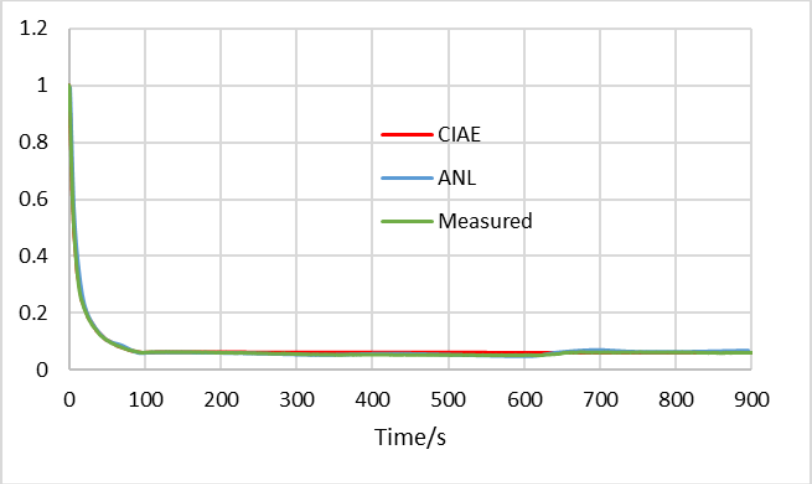


*Fig.8 Nominalized inlet flow of results for CIAE，ANL and experiment measured*

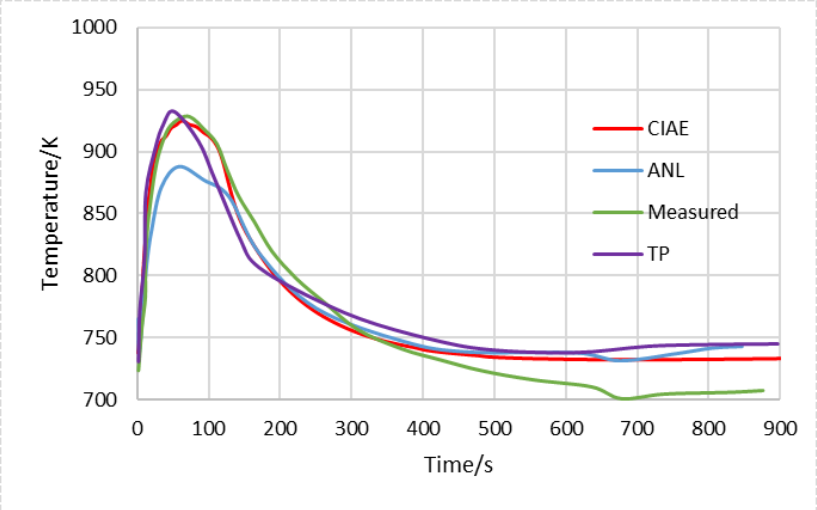

*Fig.9 Outlet temperature of results for CIAE，ANL, TP and experiment measured*

## 5. Parameter case study

As can be seen from the above analysis, the coolant density change reactivity feedback has an important impact on the process of accident. Therefore, it is necessary to analyze the sensitivity of the reactive feedback caused by coolant density change to determine its impact on the consequences of the accident.

Sensitivity analysis is divided into four cases, each case selects a different coolant density change reactivity input(include the nominal case), the specific cases introduction are as follows:

Table.5 Table of Sensitivity Analysis Conditions

| Case No. | Parameter description |
|---|---|
| Case-1 | Coolant density change reactivity is reduced by 50% |
| Case-2 | Nominal case |
| Case-3 | Coolant density change reactivity is increased by 50% |
| Case-4 | Coolant density change reactivity is increased by 100% |

Fig.10 shows the nominalized power for case-1, case-2, case-3 and case-4. It can be seen from the figure that the variation trend of the nominalized power is very consistent with the four calculation cases. When the reactivity of sodium density change decreased, the nominalized power decreased more rapidly, and when the sodium vacuolar reactivity increased, the nominalized power decreased more slightly. When the sodium density change reactivity is reduced by half, the nominalized power for case-1 increases by up to 13.21% than case-2(nominal case). When the sodium density change reactivity is increased by half, the nominalized power for case-3 decreases by up to 8.90% than case-2(nominal case). When the sodium density change reactivity is doubled, the nominalized power for case-4 decreases by up to 15.32% than case-2(nominal case). The nominalized power eventually converged, with a difference of $10^{-3}$ orders of magnitude.

Fig.11 shows the net reactivity change for case-1, case-2, case-3 and case-4. It can be seen from the figure that the variation trend of the net reactivity is consistent with the expectation. When the reactivity of sodium density change decreased, the net reactivity decreased, and when the sodium density change reactivity increased, the net reactivity increased. When the sodium density change reactivity is reduced by half, the net reactivity for case-1 decreases by up to 10.49% than case-2(nominal case). When the sodium density change reactivity is

increased by half, the net reactivity for case-3 increases by up to 8.48% than case-2(nominal case). When the sodium density change reactivity is doubled, the net reactivity for case-4 increases by up to 15.53% than case-2(nominal case).

Fig.12 shows the peak temperature of fuel in the hottest channel for case-1, case-2, case-3 and case-4. It can be seen from the figure that the variation trend of the fuel temperature is very consistent with the net reactivity changes. When the reactivity of sodium density change decreased, the peak fuel temperature increased, and when the sodium density change reactivity increased, the net reactivity increased. When the sodium density change reactivity is reduced by half, the fuel temperature for case-1 increases by up to 35.31(3.9%) than case-2(nominal case). When the sodium density change reactivity is increased by half, the fuel temperature for case-3 decreases by up to 24.23K(2.68%) than case-2(nominal case). When the sodium density change reactivity is doubled, the fuel temperature for case-4 decreases by up to 41.97K(4.64%) than case-2(nominal case). As the EBR-II reactor uses metallic fuel, metallic fuel has good thermal conductivity, the variation trend of the temperature for fuel, cladding and coolant under different calculation cases are similar, so there are no details about the temperature of cladding and coolant. Overall, when the reactivity brought by the coolant density change decrease, the fuel and cladding do not melt, and no coolant boiling occurs.

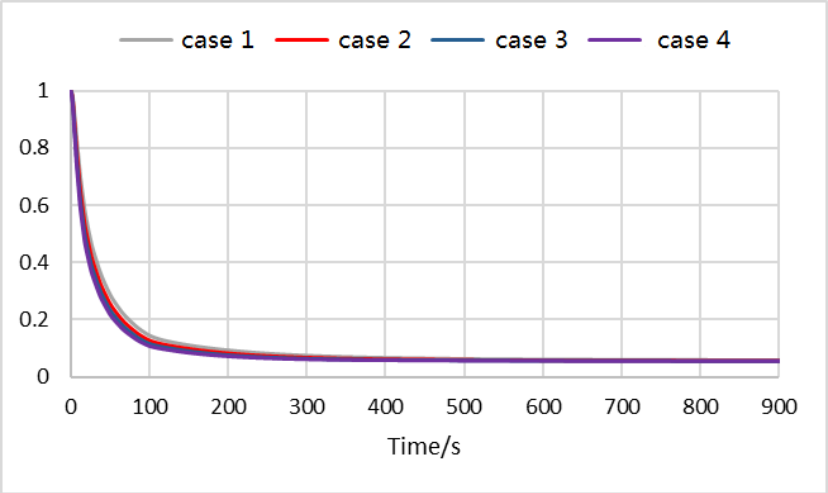


*Fig.10 The nominalized power for case-1, case-2, case-3 and case-4*

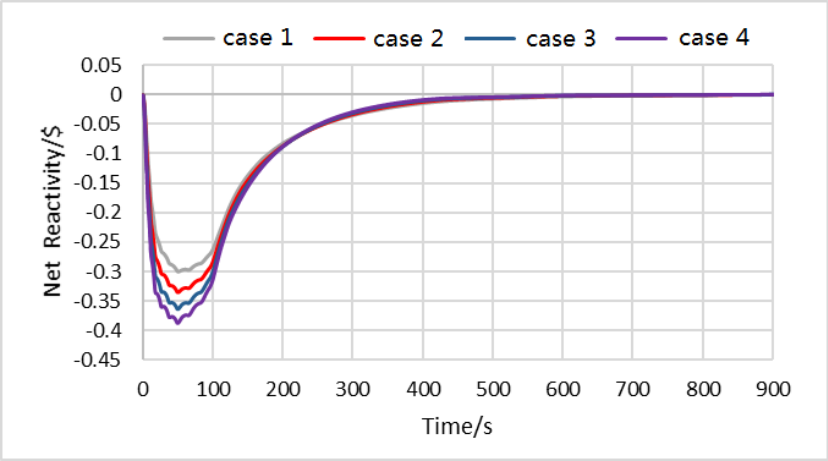


*Fig.11 Reactivity change for case-1, case-2, case-3 and case-4*

As can be seen from the above analysis, when the sodium density change reactivity is reduced by half, increased by half and doubled, process of accident is basically the same with the nominal case. The variation of net reactivity and power are both within 15%, variation of temperature for fuel(cladding and coolant) are within 5%.

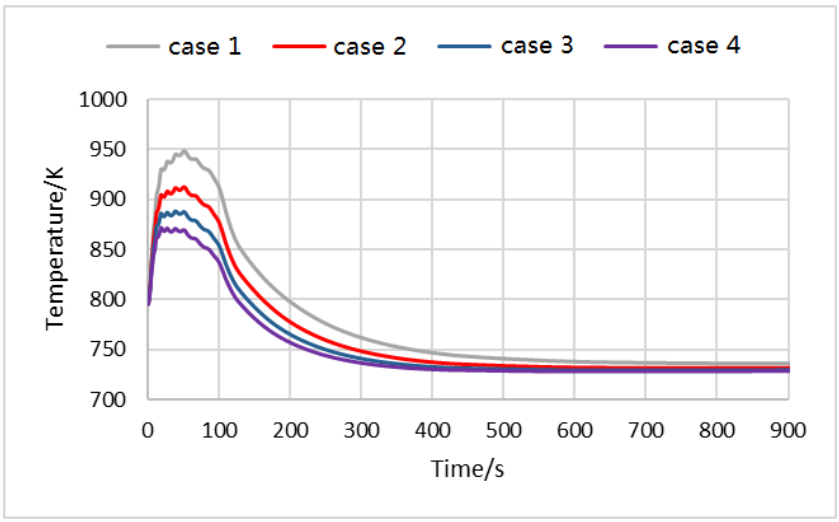


*Fig.12 The peak temperature of fuel in the hottest channel for case-1, case-2, case-3 and case-4*

## 6. Conclusion

In this paper, the SHRT-45R of EBR-II reactor is modeled with the SAS4A code, and the unprotected loss of flow accident is calculated and analyzed. The following conclusions can be drawn:

The calculated results of this paper are in good agreement with the results of ANL and experimental measurements, through which the correctness of the calculation model and calculation scheme are verified.

After ULOF accident occurs, small-scale metallic fuel sodium cooled fast reactor can use their own negative feedback to reduce power, and the temperature of the fuel, cladding and coolant is finally stabilized at a low level, fuel and cladding do not melt during the accident, there is a large margin from boiling for coolant, which verifies the inherent safety of the metallic fuel sodium cooled fast reactor.

In all negative feedback, reactivity feedback caused by sodium density change contributes the most. Because the size of EBR-II reactor is small, when the temperature of the coolant increases, the sodium density decreases, bringing the neutron leakage rate increases, which introduces a larger negative feedback.

Sensitivity analysis of the negative feedback caused by coolant density change is carried out, which shows that sodium density change reactivity has little effect on the accident process within a certain range.

## REFERENCES

[1] XU Mi. Fast reactor development strategy targets study in China[J]. Chinese Journal of Nuclear and Engineering, 2008, 28(1): 12-20.

[2] Sheng Zhaoqi. metallic Fuels and Blankets in Liquid-metallic Fast Breeder Reactors[J]. Nuclear Power Engineering, 1988, 9(4): 33-41.

[3] R.Wigeland, J.Cahalan. Fast Reactor Fuel Type and Reactor Safety Performance[A].Proceedings of Global 2009.Paris,2009,9.

[4] YU Baoan. Inherent Safety of Sodium Cooled Fast Reactor[J]. Nuclear Power Engineering, 1989, 10(4): 90-96.

[5] Sumner T. W T Y. Benchmark Specifications and Data Requirements for EBR II Shutdown Heat Removal Tests SHRT 17 and SHRT 45R[J]. Nuclear Engineering Division Argonne National Laboratory, ANL-ARC-226-(Rev 1).

[6] E. E. Feldman and D. Mohr. Unprotected loss-of-heat sink simulation in the EBR-II plant. EBR-II Division Argonne National Laboratory Argonne, Illinois 60439[J].

[7] M.G. Stevenson, et al., Current Status and Experimental Basis of the SAS LMFBR Accident Analysis Code System, Proc. of the Fast Reactor Safety Meeting, 1974.

[8] A.M. Tentner, et. al., The SAS4A LMFBR Whole Core Accident Analysis Code - Proc. of the International Meeting on Fast Reactor Safety Technology,

Knoxville, Tennessee (Apr. 1985).